Sedimentary Geology 468 (2024) 106675

Contents lists available at ScienceDirect

Sedimentary Geology

journal homepage: www.elsevier.com/locate/sedgeo

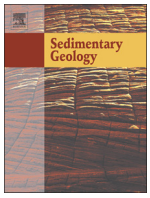

Island accretion within a degraded reef ecosystem suggests adaptability to ecological transitions

Yannis Kappelmann [a,b,*], Meghna Sengupta [a], Thomas Mann [a,c], Marleen Stuhr [a], Dominik Kneer [a], Jamaluddin Jompa [d], Hildegard Westphal [a,b]

[a] Leibniz Centre for Tropical Marine Research (ZMT), Bremen, Germany
[b] University of Bremen, Department of Geosciences, Bremen, Germany
[c] Federal Institute for Geosciences and Natural Resources (BGR), Hannover, Germany
[d] Research and Development Center for Marine, Coastal, and Small Islands, Hasanuddin University (UNHAS), Makassar, Indonesia

ARTICLE INFO

Article history:
Received 5 February 2024
Received in revised form 2 May 2024
Accepted 8 May 2024
Available online 15 May 2024

Editor: Dr. Giorgio Basilici

Keywords:
Coral reef degradation
Reef islands
Sea-level change
Ecosystem services
Anthropogenic stress
Carbonate sediment
Holocene
Spermonde Archipelago

ABSTRACT

Reef islands, elevated only a few meters above sea-level and restricted in area, are not only confronted with rising sea-levels, but the surrounding reef ecosystems, which are the only source of sediment maintaining those islands, are threatened by global (e.g. ocean warming and acidification) and local anthropogenic (e.g. pollution and destructive fishing methods) stressors affecting many tropical coastal areas. These stressors can increase coral mortality and lead to shifts from coral- to macroalgal-domination, likewise altering the production of skeletal carbonate sediment and ultimately endanger the physical persistence of reef islands. Here we study the evolution of an Indonesian reef island that has been inhabited since the 20th century. By analyzing the sedimentary record covering the last 5800 years from sediment cores taken on the island, we study the formation processes during the Holocene. For understanding the spatial dynamics, we compare the sediment record of the past decades with observations from satellite imagery data. Two shifts in the sedimentological composition over time point to alterations in the sediment-supplying reef ecosystems. The first sedimentological shift occurred from 3900 years BP on, shortly before the initial formation of the island, when the skeletal composition was diversified, presumably reflecting the modification of the reef ecosystem following a sea-level drop. A second sedimentological shift in the youngest sediments is marked by increased proportions of the calcifying green algae *Halimeda*, indicating that the reef ecosystem has shifted toward algal-domination, presumably reflecting increasing anthropogenic pressure. Of significance, shoreline change analysis reveals that the island is in an accreting state and has grown by 13 % in surface area over the past 24 years. Our findings suggest that the compositional alterations in sediment supply did not destabilize the reef island, and underline the adaptive potential of these landforms.

1. Introduction

Widespread degradation of tropical coral reef ecosystems is currently observed globally, caused by temperature-driven coral bleaching events as well as regional anthropogenic pressures such as pollution, extensive and destructive fishing methods, or mining of coral reefs for infrastructural use (Edinger et al., 1998; Hoegh-Guldberg et al., 2007; Perry et al., 2013). Degradation impairs the natural ecosystem services provided by coral reefs, which also include the production of carbonate frameworks and sediments nourishing coastal landforms such as reef islands (Westphal et al., 2022). Reef islands, formed primarily of skeletal remains of marine organisms from coral reefs and related ecosystems, are low-lying landforms, rising rarely more than a few meters above mean sea level (Stoddart and Steers, 1977; Perry et al., 2011; Kench et al., 2020). They are inherently dynamic landforms in that they largely consist of unconsolidated sediments that allow waves to rework shoreline deposits, modifying the position of the shoreline on a seasonal scale (e.g. as response to monsoon winds) or on a multiannual scale (e.g. seasonal El Niño events), which ultimately also leads to the loss of parts of the sediment from the island peripheries to deeper waters (Kench et al., 2009; Kench and Mann, 2017; Cuttler et al., 2020). In a stable dynamical state, such erosional deficits in the sediment budget are compensated by the constant production of skeletal material by the ecosystems, hence preventing reef islands from erosion in the long term (Perry et al., 2011). However, with reef degradation and the additional impact of rising sea level, reef islands face an uncertain prospect for their future

* Corresponding author at: Leibniz Centre for Tropical Marine Research (ZMT), Bremen, Germany.
E-mail address: yannis.kappelmann@leibniz-zmt.de (Y. Kappelmann).

https://doi.org/10.1016/j.sedgeo.2024.106675

as habitable space for humans (Woodroffe et al., 2017; Storlazzi et al., 2018).

Reef islands in the Pacific and the Indian Oceans have primarily formed since the mid-Holocene, over the past ~5000 years (Woodroffe et al., 1999; Woodroffe and Morrison, 2001; McKoy et al., 2010; Kench et al., 2012), largely from coral fragments, which underlines their pivotal role in island building and maintenance (Perry et al., 2011). While storms produce mostly coarse coral rubble, bioerosion of grazing parrotfish contributes predominantly sand-sized fractions to the sediment budget (Scoffin, 1993; Perry et al., 2015; Morgan and Kench, 2016a). Due to their strong skeletal structure, coral fragments endure abrasion effectively and thus persist as long-lasting components for coastal landforms (Perry et al., 2011; Ford and Kench, 2012). As a consequence of reef degradation, transitions of coral- to macroalgal-dominated reef ecosystems have recently been observed in several reefs and are projected to increase in the future (Hoegh-Guldberg et al., 2007; Janßen et al., 2017; Perry et al., 2020; Sari et al., 2021; Fukunaga et al., 2022). Evidently, such shifts will affect the reef sediment production and budgets, also impacting the sediment characteristics and supply to islands (Perry et al., 2013; Liang et al., 2016). In macroalgal-dominated reefs, considerable production of carbonate is attributed to increased settlement of red crustose coralline algae (CCA) and green algae (*Halimeda*), of which the latter are directly incorporated in the sediment budget upon death of the algae (Perry et al., 2020; Huntington et al., 2022). The elevated sediment production of *Halimeda* in the vicinity of reef islands may, however, not necessarily be reflected in high proportions of the island deposits, as the platy and porous structure of the segments allows fast transport to the island margins, but also can lead to quick breakdown in their high-energetic littoral zones (Ford and Kench, 2012; Wizemann et al., 2015; Morgan and Kench, 2016b; Perry et al., 2020).

Increasing numbers of studies are analyzing satellite imagery to determine reef island dynamics in response to the ongoing sea-level rise and changing climatic conditions, contributing to a better understanding and projection of the response of such islands (Webb and Kench, 2010; Husband et al., 2023; Sengupta et al., 2023). A comprehensive review by Duvat (2018) points out that most reef islands in the Pacific and Indian Oceans have remained stable over the last decades. However, the decadal-scale interplay between ecological shifts and island dynamics is still not well constrained, in part because such ongoing changes have mainly been reported only recently (Hoegh-Guldberg et al., 2007; Browne et al., 2021). The integration of recent sedimentological data with satellite image analyses of shoreline dynamics is as yet sparse, however needed to understand the decade to century scale dynamics of reef islands. In particular, the analysis of satellite imagery around actively accreting island margins can provide evidence of the timing of deposition and thus help to examine the connection between island growth and possible facies shifts in these sediments.

Here we contribute to the understanding of the relationship between shifts in the sediment producing biota of reef ecosystems and reef island evolution by investigating an Indonesian reef island from offshore Sulawesi, Indonesia, that has been used by humans intensively since the beginning of the 20th century. The analysis of the sedimentological composition of radiocarbon-dated sediment cores allows us to reconstruct the Holocene formation over the past 5800 years cal BP in the context of the varying ecological background. Through analysis of remote sensing data from recent decades (1999–2023), we link the reef island shoreline evolution to the status of the adjacent local coral reef ecosystem.

2. Regional setting

The Spermonde Archipelago is a land-attached carbonate shelf in the Coral Triangle, between the mainland of SW Sulawesi to the east and the Strait of Makassar to the west (Fig. 1A, B). Around 120 reef islands across the shelf provide habitable space for approximately 50,000 inhabitants (Glaser et al., 2015; Kench and Mann, 2017). The Spermonde Archipelago is bordered by a reef rim that forms a topographic barrier protecting the inner shelf from open ocean conditions. A steep slope drops into the up to 2500 m deep Strait of Makassar that funnels the Indonesian Throughflow waters from the Pacific Ocean southward into the Indian Ocean (Hall et al., 2009; Gordon et al., 2019). The seasonally reversing monsoon as a dominating wind system strongly influences the physical and ecological dynamics, including reef and reef island development (Umbgrove, 1928; Wijsman-Best et al., 1981; Kench and Mann, 2017; Kappelmann et al., 2023). Strong NW winds during boreal winter generate waves on the Strait of Makassar that expose the outer rim to high hydrodynamic energy. The SE winds during boreal summer are damped by the mountainous hinterland of the Sulawesi mainland and are therefore weaker, yet lead to seasonal upwelling in the Strait of Makassar on the outer rim (Ilahude, 1970, 1978; Hoeksema, 2012).

During the Holocene at around 5700 years cal BP, a highstand with a mean relative sea-level (MSL) of 0.5 m above modern sea-level has been recorded, while the modern MSL was reached around 4200 years cal BP (Mann et al., 2016; Bender et al., 2020). Little is known about island formation in the Spermonde Archipelago, however, the mid-shelf island Barrang Lompo has been shown to have formed during the Holocene on top of an infilled lagoon (Kappelmann et al., 2023). Kappelmann et al. (2023) showed that this process was slowed-down during the sea-level highstand, and the later infill took place only after the contemporary dominant NW monsoon pattern had established, following a time of weaker monsoon in the early Holocene (Mohtadi et al., 2011; Ding et al., 2013).

In our present study, we investigate the island Langkai (Fig. 1C) that is located on the southern rim of the Spermonde Archipelago and has an area of 23 ha (2023) with an elevation of ~1.8 m above MSL. Infrastructure is concentrated in the northern area of the island. In the center of the island is a public sports field, which according to the local community marked the southern shoreline in the early 20th century (Figs. 1C, 3B).

3. Material and methods

3.1. Field methods

Five push cores were recovered along a transect from the northern to the southern shoreline of Langkai in 2016 (Fig. 1C). The probes of 1 m length with an internal liner with a diameter of at least 28 mm were pushed in the same hole repeatedly to reach a maximum depth of 8 m. Sediment samples were taken from the lower 10 cm of each of the 1 m-probe intervals (n = 22). Sample coding indicates the core number (LK1 to LK5) and depth below surface in meters (e.g. LK1-3 indicates 3 m below surface). In the northern location LK1, a maximum drilling depth of 8 m below surface was reached while at all other locations, at 4 m below surface, penetration was obstructed by a solid layer. Nine additional cores were taken in August 2021 with a hand-held 120 cm long Auger corer at 31 locations in the intervals between the push cores in the existing N–S transect, and 22 cores were taken along a new W–E transect (Fig. 1C). Analyses were undertaken on sediment of the lowermost 10 cm of the cores. The maximum depth of the Auger corer of 110–120 cm below surface was reached in most cores, while for nine cores, lithified layers restricted coring to shallower depths (see Kappelmann et al., 2024 for locations and depths).

3.2. Lab methods

Sediments were dry-sieved into phi fractions according to the classification by Wentworth (1922) using GRADISTAT v9.1 for statistics (Blott and Pye, 2001). For determining the origin of the sediment grains, the gravel (>2 mm), very coarse sand (2–1 mm), coarse sand (1–0.5 mm), and medium sand (0.5–0.25 mm) fractions were analyzed using a digital microscope. We identified n = 100 grains per fraction (n =

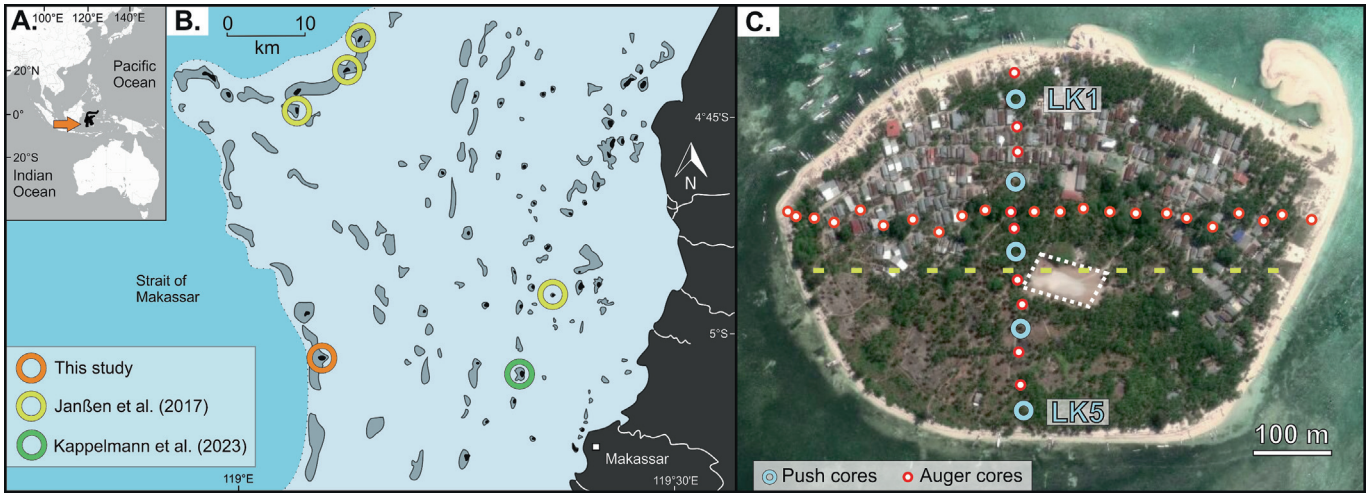

Fig. 1. A. Study area in Indonesia with Sulawesi marked in black and orange arrow indicating the Spermonde Archipelago; B. Spermonde Archipelago between the Sulawesi mainland and the Strait of Makassar, shallow reefs marked in gray and reef islands in black; based on Kench and Mann (2017); C. study island Langkai with locations of five deep push cores and 31 shallow Auger cores along a N–S transect and an E–W transect. Yellow dashed line marks the southern shoreline in the late 19th century as communicated by the local community; the white rectangle marks the sport field.
(Imagery Copyright 2021 Maxar Technologies Inc.)

400 per sample), analogous to comparable studies (East et al., 2016; Janßen et al., 2017). The following component categories were identified: corals, CCA, *Halimeda*, gastropods, and foraminifers. The group of bivalves, echinoderms, bryozoans and serpulids was summarized as "others" for their insignificant abundances. Furthermore, we noted cemented grains ("aggregates") and non-identifiable grains ("bioclasts"). As this study focuses on interpreting the ecological background, these grains were not included in the count of $n = 100$ per fraction.

Radiocarbon ages were determined on bulk sediment by extracting a minimum quantity of 500 mg from the coarse sand fraction of 20 samples selected in a spatially representative grid by the Poznan Radiocarbon Laboratory, Poland. We corrected the conventional radiocarbon ages using the online interface OxCal v4.4 (Bronk Ramsey, 2009) and implemented the Marine20 curve (Heaton et al., 2020). As regional marine reservoir correction we chose $\Delta R = 0 \pm 0$ as in other studies from the Spermonde Archipelago (Bender et al., 2020; Kappelmann et al., 2023). We use the mean calibrated age (termed *years cal BP*) for the present study.

3.3. Shoreline analysis

Shoreline positions were analyzed on the basis of 11 satellite images covering the time interval from 1999 to 2023 that were imported and georeferenced in ArcGIS (Version 10.8.2). The satellite images were obtained from the United States Geological Survey, Esri & Maxar Technologies Inc., Airbus DS and Planet Labs PBC (see Kappelmann et al., 2024 for exact list of images, acquisition dates and sensors). We used the edge of vegetation as shoreline proxy, which, unlike the toe-of-beach, is largely unaffected by seasonal and tidal fluctuations, and is commonly used for multidecadal analysis (Webb and Kench, 2010). Shorelines were manually digitized from each image at a uniform scale by a single operator. We then used the Digital Shoreline Analysis System (Thieler et al., 2009) to cast digital transects at intervals of 5 m from an onshore baseline and applied a confidence interval of 2σ (95.5 %) for the calculation of uncertainty in shoreline change statistics. We use the Net Shoreline Movement (NSM) and End Point Rate (EPR) in this study, that provide a measure of the distance between the oldest and latest recorded shorelines and a rate of change by normalizing the distance by elapsed time, respectively. A total of 306 digital transects were cast, where transects showing positive upper and lower intervals of EPR were classified as significant accretion, negative upper and lower intervals as showing erosion, and the remaining classified as stable. The net migration of the island footprint on the reef platform was measured as the distance between temporally consecutive island centroids.

Additionally, a 1:100,000 scale hydrographic survey map from 1897 of the archipelago was obtained from the National Archives in The Hague, Netherlands. Due to the high uncertainty in spatial referencing, this map was not used to quantify changes in area, however, it serves as a reference for examining the configuration and footprint of the vegetated island core from ~125 years ago.

4. Results

4.1. Sedimentological characteristics

The unconsolidated subsurface sediments retrieved from below MSL, i.e. push cores from 2 m depth or deeper (Fig. 2A), differ markedly in composition and texture from those taken from above MSL, i.e. the uppermost samples from the push cores and the Auger cores (Fig. 2B, C). The samples from below MSL consist of gravel-rich sediments. At the basis, push cores show a pronounced dominance of coral fragments; in the northernmost core LK1 (LK1-8 and LK1-6) they consist entirely of coarse coral fragments (Fig. 2A; see Supplementary Tables S1 for additional information). These gravels are overlain by sand-sized sediments, that are also dominated by coral fragments, but have a more diverse composition in the samples LK1-5 to LK1-2 in which coral is the dominant (50 to 59 %) component. *Halimeda* and gastropods represent each >10 %, while CCA and foraminifera are minor constituents with <10 %. The cores LK2, LK3 and LK4 show similar trends over depth (Fig. 2A). Their gravelly basal samples (LK2-4, LK3-4 and LK4-4) contain predominantly coral fragments (82 to 92 %), and minor components are CCA (4 to 7 %) and gastropods (3 to 6 %). Above, coral-dominated (52 to 68 %), gravel-sand deposits prevail with subordinated contributions from gastropods (8 to 17 %), *Halimeda* (6 to 12 %) and CCA (5 to 12 %), while foraminifera are usually rare (1 to 9 %). In the southernmost core LK5, the three deepest samples (LK5-4, LK5-3 and LK5-2) contain gravelly sediment composed of coral (64 to 68 %), as well as CCA (9 to 13 %), gastropods (8 to 12 %) and *Halimeda* (7 to 11 %).

In the shallow samples from above MSL, sand-sized grains prevail (Fig. 2B, C). These are primarily formed by coral, *Halimeda* and gastropods, of which the first two vary most notably in contribution. Along the N–S transect (Fig. 2B), the samples close to the northern shoreline (A1 and A2) are dominated by coral and *Halimeda* (both >30 %), with subordinate contributions from gastropods (16 to 26 %) and

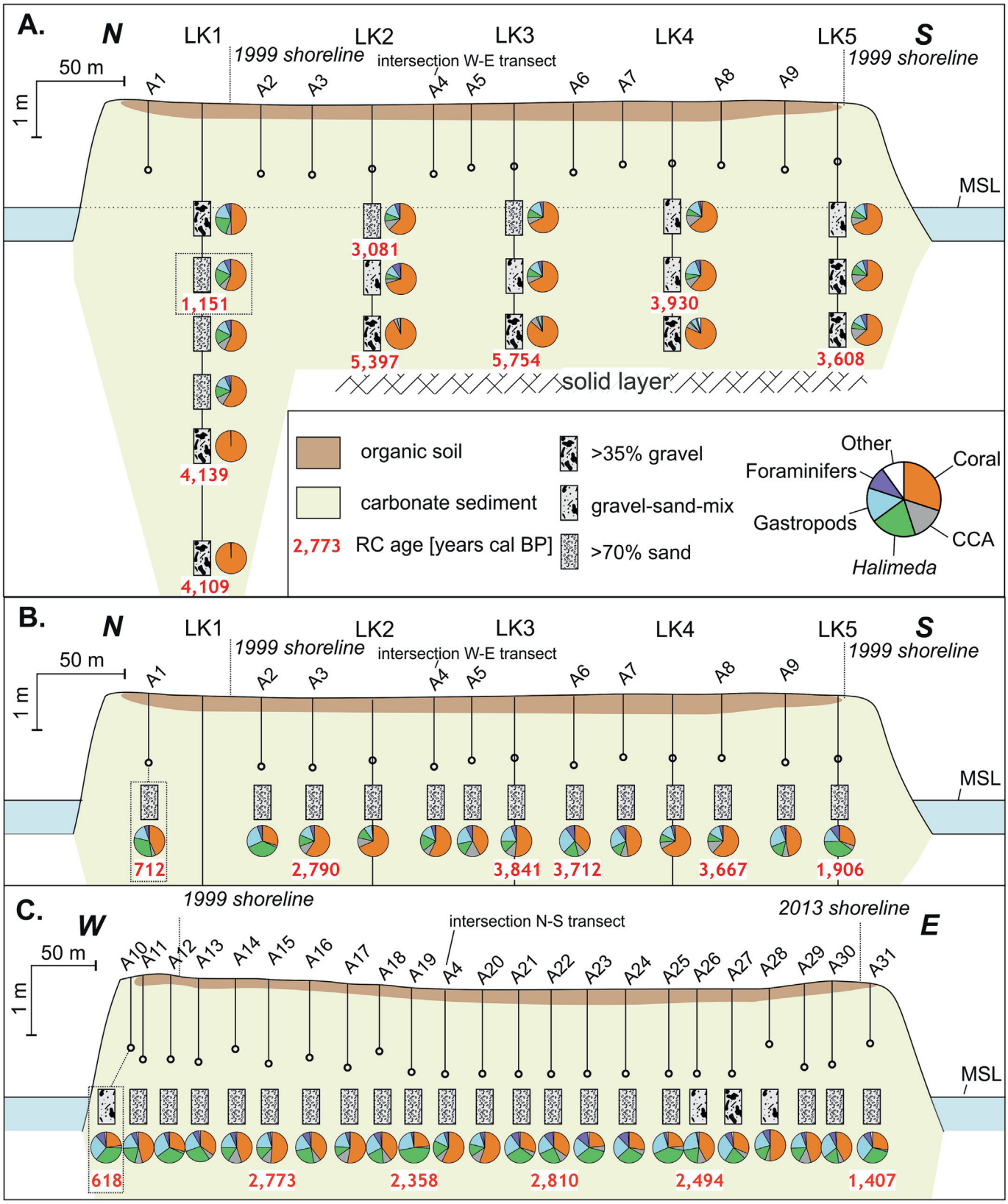

Fig. 2. Sediment profiles across the two transects on Langkai with sediment texture, sediment composition and radiocarbon ages. A. N–S transect below MSL with deep push cores LK1 to LK5. B. Shallow push cores and Auger cores A1 to A9 from above MSL along the N–S transect. C. E–W transect with Auger cores A10 to A31 above MSL. Dashed lines indicate minimum extension of shorelines as observed from satellite image data since 1999. The detailed skeletal and textural composition of each sample in this figure can be found in the Supplementary Tables S1.

foraminifera (4 to 5 %). From sample A3 southward to A9, coral fragments (38 to 68 %) are the main constituents, and other components such as gastropods (8 to 28 %), *Halimeda* (9 to 22 %), CCA (7 to 16 %) and foraminifera (1 to 9 %), have varying proportions. The southernmost shallow sample (LK5-1) is, similar to the northern samples, mainly composed of *Halimeda* (39 %) and coral (30 %).

Table 1
Conventional and calibrated radiocarbon (RC) ages of 20 selected samples.

Lab code	Sample ID	Material analyzed	Conventional RC age [years BP]	Calibrated RC age range, 95.4 % probability [years cal BP]	Mean calibrated RC age [years cal BP]
Poz-154832	LK1-3	Bulk sediment	1755 ± 30	1283–1008	1151
Poz-154833	LK1-6	Coral fragments	4230 ± 35	4335–3955	4137
Poz-154836	LK1-8	Coral fragments	4210 ± 35	4295–3919	4109
Poz-154834	LK2-2	Bulk sediment	3395 ± 30	3250–2908	3081
Poz-154835	LK2-4	Bulk sediment	5225 ± 35	5562–5259	5397
Poz-154789	LK3-1	Bulk sediment	4010 ± 30	4017–3665	3841
Poz-154838	LK3-4	Bulk sediment	5565 ± 35	5901–5594	5754
Poz-154241	LK4-3	Bulk sediment	4075 ± 35	4110–3744	3930
Poz-154239	LK5-1	Bulk sediment	2440 ± 30	2066–1741	1906
Poz-154240	LK5-4	Bulk sediment	3830 ± 35	3791–3445	3608
Poz-160367	A1	Bulk sediment	1320 ± 30	855–575	712
Poz-160369	A3	Bulk sediment	3150 ± 30	2940–2664	2790
Poz-160370	A6	Bulk sediment	3910 ± 30	3880–3546	3712
Poz-160417	A8	Bulk sediment	3875 ± 30	3830–3496	3667
Poz-160442	A10	Bulk sediment	1220 ± 30	731–506	618
Poz-160441	A15	Bulk sediment	3135 ± 30	2925–2635	2773
Poz-160371	A19	Bulk sediment	2795 ± 30	2530–2169	2358
Poz-160445	A22	Bulk sediment	3170 ± 30	2955–2685	2810
Poz-160444	A26	Bulk sediment	2900 ± 30	2671–2336	2494
Poz-160445	A31	Bulk sediment	2010 ± 30	1536–1280	1407

Along the W–E transect (Fig. 2C), the samples close to the western (A10 to A13) and eastern (A31) shoreline contain high proportions of coral (23 to 46 %), *Halimeda* (21 to 36 %) and gastropods (18 to 29 %). Farther from the shorelines, the samples A14 to A20 (40 to 55 % coral), with the exception of A19 that has the highest content of *Halimeda* in our data (46 %), as well as A26 to A30 (31 to 50 % coral) show dominating coral fragments, gastropods (20 to 31 %) and Halimeda (15 to 22 %). The samples A21 to A25 contain mainly *Halimeda* (25 to 40 %) and coral (23 to 35 %).

4.2. Radiocarbon ages

A total of 20 radiocarbon ages were determined, 14 for the N–S transect and 6 for the W–E transect (Table 1 and Fig. 2). The radiocarbon ages from the deep section of the northernmost core, LK1-8 and LK1-6, reveal similar ages of 4109 and 4139 years cal BP (Fig. 2A). The oldest ages in our data set are found in the basal samples of the central cores in LK3-4 (5754 years cal BP) and LK2-4 (5397 years cal BP). Overlying sediments on the N–S transect from the center toward south range from 3930 to 3608 years cal BP (Fig. 2A). Sample LK3-1 has the oldest radiocarbon date above MSL with 3841 years cal BP. Along the W–E transect, we find comparably younger ages around the island center, ranging from 2358 to 2810 years cal BP (Fig. 2B). The youngest samples of each transect are recorded close to the recent shorelines with 712 and 1906 years cal BP on the N–S transect and 618 and 1407 years cal BP on the W–E transect. Also, the sample LK1-3 (1152 years cal BP) in the northernmost core has a relatively young age.

4.3. Shoreline analysis

A total of 306 analyzed digital transects reveal that accretion was significant in 84.97 % of the transects, whereas 14.05 % eroded and 0.98 % remained stable between 1999 and 2023 (Fig. 3). The prevailing accretion resulted in a marked expansion of the island area to 22.95 ha in 2023, indicating a net increase of 2.61 ha (12.8 %) since the start of the 21st century (Fig. 3E). The highest rates of shoreline advance are reported along the north and northwest margins (~60 m), as well as in the south (~30 m), where mean annual accretion rates are well above 1.0 m year^{-1} (Fig. 3C). The eastern part of the island shows widespread erosion, where the shoreline retreated by ~70 m. Intermediate accretion and subsequent erosion are found in the northeast of Langkai, however over the time analyzed this part of the island is characterized by net accretion. The imbalance in the magnitude of erosion and accretion around the island margin led to the migration of the island footprint on the reef platform, with the centroid of Langkai having moved by 30.92 m toward the NW within the last 24 years (Fig. 3C).

5. Discussion

5.1. Holocene island formation

5.1.1. Mid-Holocene highstand sedimentation

The deepest samples in the center of the island (LK2-4, LK3-4 and LK4-4), taken from depths of 2.2 m below modern MSL, consist of coral-rich (~82 to 92 %) sediments, with minor contributions of CCA (~4 to 7 %) and gastropods (~3 to 6 %). These basal sediments are dated to 5754 and 5397 years cal BP (LK3-4 and LK2-4), thus indicating that the oldest sediments in our study were deposited during a mid-Holocene sea-level highstand that was reached at 5700 years cal BP (Mann et al., 2016; Bender et al., 2020). The dominance of coral fragments with minor contributions from CCA and gastropods in the sediment suggests that the variety of carbonate secreting reef organisms was limited. Similar sediments are found in Holocene reefs from Japan and are thought to have formed during vertical reef growth, i.e. catch-up, during rising sea-level (Neumann and Macintyre, 1985; Yamano et al., 2001). The core depth and the solid layer beneath imply that the upward growth of the solid coral framework beneath the recent island stopped around 2.2 m below MSL and the island later formed on this foundation (Fig. 4H1).

5.1.2. Mid-Holocene post-highstand sedimentation

The sediments that overlay the basal deposits in the cores LK2 to LK4 and the sediments in the southern core LK5 have notably younger radiocarbon dates (e.g. LK4-3 with 3930 years cal BP and LK 5-4 with 3608 years cal BP), therefore indicating that the these were deposited after sea-level had fallen to the contemporary level by 4200 years cal BP (Mann et al., 2016; Bender et al., 2020). The sediments are sand–gravel mixtures, composed of more diverse skeletal assemblages than below (Fig. 2A), with dominant coral and contributions from gastropods, CCA, *Halimeda* and foraminifers, thus indicating an ecological transition in the sediment producing biota. Similar transitions are known from reef islands in the Great Barrier Reef, Australia and the Maldives, where post sea-level fall sedimentation was characterized by increased proportions of e.g. foraminifers and mollusks (Yamano et al., 2000; Kench et al., 2020). As the MSL affects the ecological reef zones by steering the hydrodynamic energy (Done, 1982), the sea-level fall likely promoted the development of a low-energetic backreef environment, in which foraminifera, *Halimeda* and gastropods found suitable habitats. The island formation initiated presumably soon after this diversification of sediment producing biota (Fig. 4H2). The sediments and radiocarbon ages in core LK1 (samples LK1-8 and LK1-6) in the north of Langkai differ from further south in that they show pure coral sediment dated to 4137 and 4109 years cal BP (Fig. 2A, Table 1), indicating that these were formed considerably later than the basal sediments in the central cores despite their greater burial depth.

5.1.3. Late Holocene sedimentation

The island sediments obtained from above MSL that were not reworked at least since 1999 (according to the shoreline analysis, see markings in Fig. 2B, C) consist of mainly sand-sized grains. The skeletal composition in these deposits shows both, coral-dominated sediments as well as mixtures with dominant coral fragments and *Halimeda*. While the increased abundance of *Halimeda* may suggest another ecological transition in the supplying ecosystems, there is no clear pattern in the spatial distribution or temporal linkage in the radiocarbon dates that would confine it. On the N–S transect the ages of the sediments

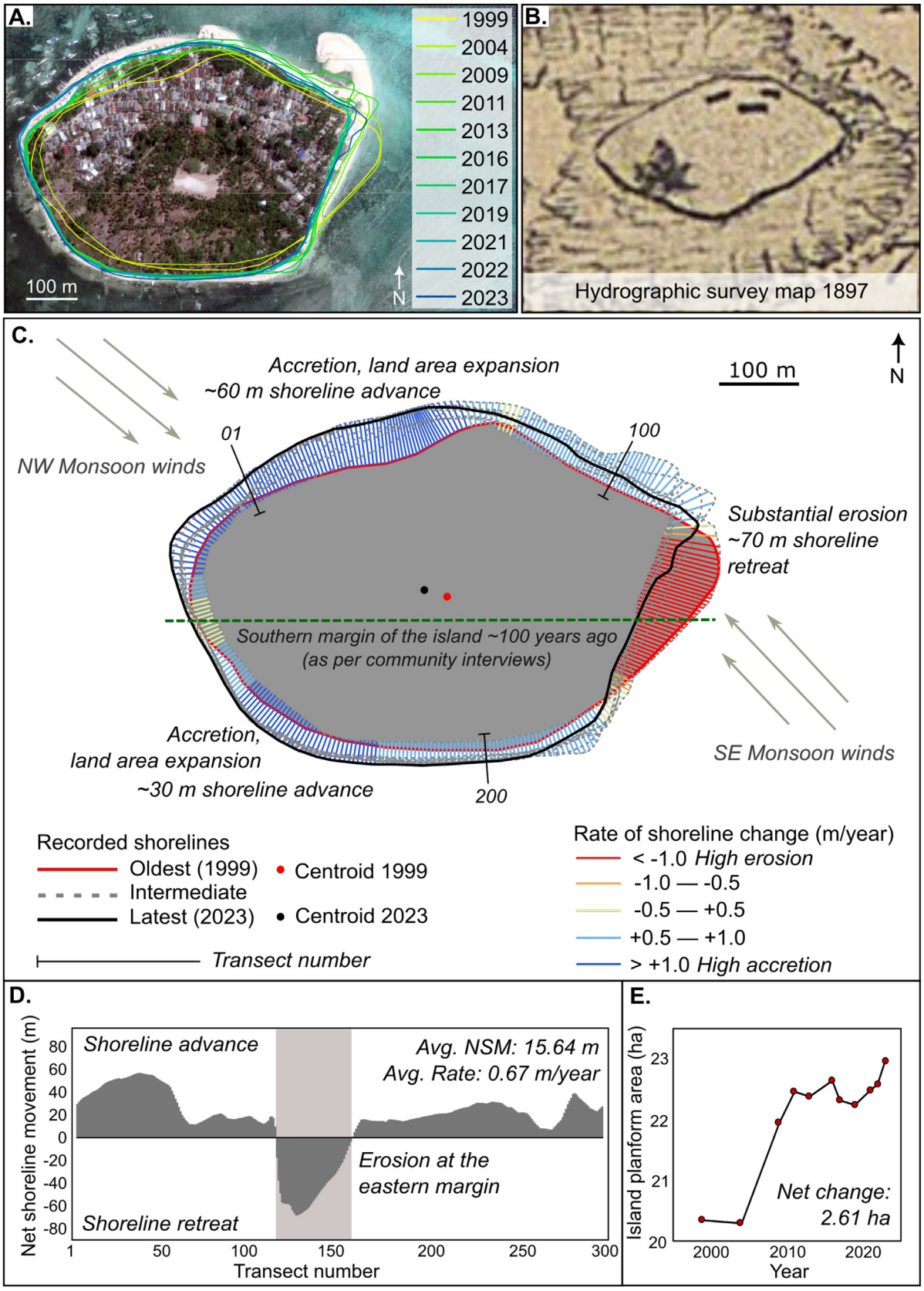

Fig. 3. Shoreline dynamics in recent decades: A. Shorelines recorded from satellite imagery between 1999 and 2023 (Imagery Copyright 2021 Maxar Technologies Inc.); B. hydrographic survey map from 1897 collected from the National Archives, The Hague, Netherlands; C. digital transect scale analysis of shoreline change rates; D. net shoreline movement; E. resulting net changes in island planform area.

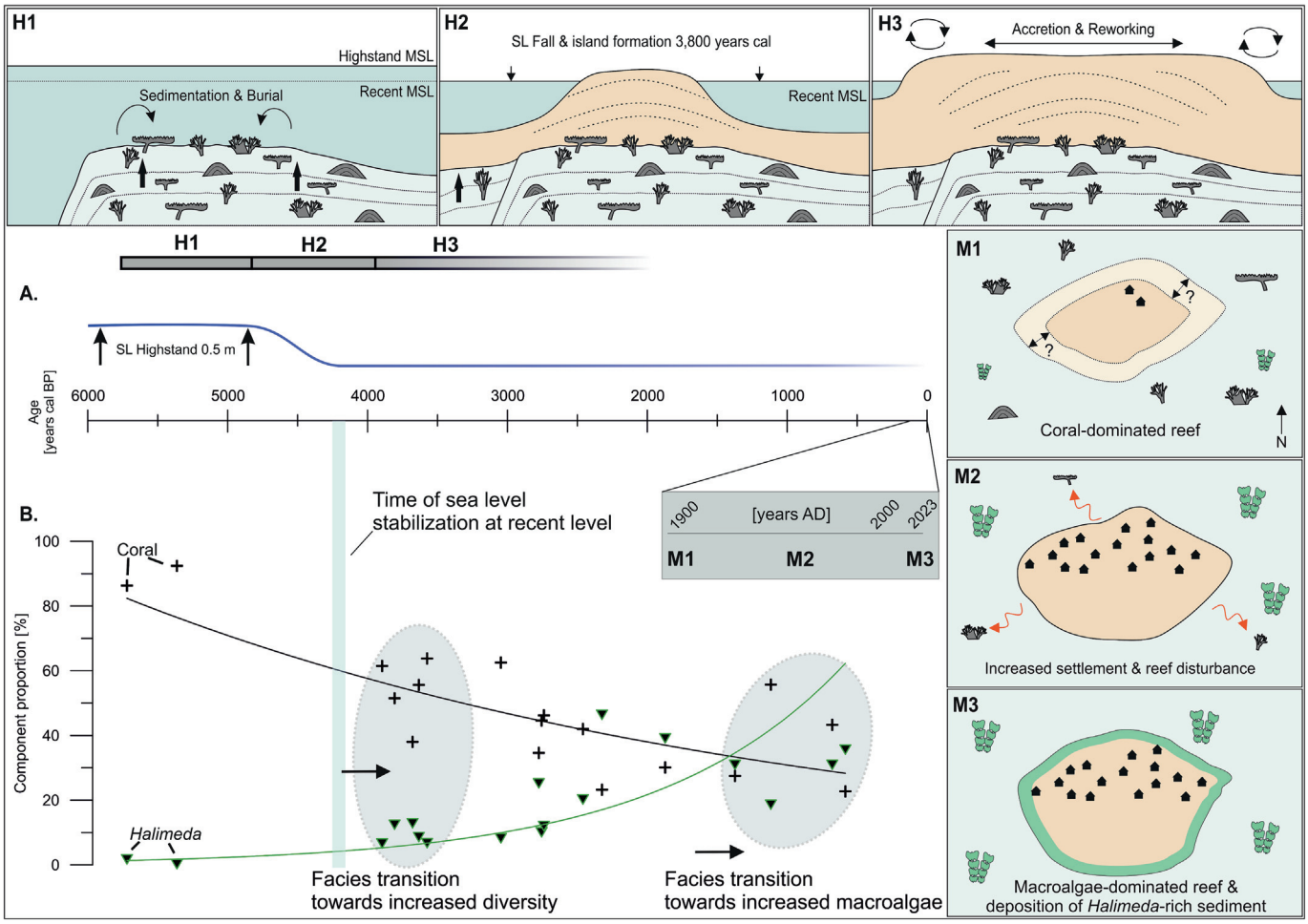

Fig. 4. A. The Holocene formation of Langkai (H1) under highstand conditions, (H2) the falling sea-level and (H3) the subsequent growth and reworking along the shorelines. Sea-level curve follows recorded data until around 3700 years cal BP from the study area (Mann et al., 2016; Bender et al., 2020). B. The relative proportions of coral and *Halimeda* in sediments that have been dated. Note that the youngest sediments contain an age bias, as explained in the following discussion. The modern island dynamics (M1–M3) present an interpretation based on the reports by the local community, the 1897 hydrographic map and the shoreline analysis, with (M1) the island shape in the late 19th century when the landform was only inhabited by few fishermen and reefs were in coral-dominated state; note that the island area is not to scale. (M2) Intensive settlement of the island in the mid 20th century and following pressure on the reefs and (M3) recent status with macroalgal-dominated reefs and their mirroring in deposition of *Halimeda*-rich sediments.

range from 3841 years cal BP (LK3-1) to 2790 years cal BP (A3), while on the W–E transect a temporal range from 2810 years cal BP (A22) to 2358 years cal BP (A19) is reported. The relatively young age in the north with 1151 years cal BP (LK1-3), indicates, however, that the slope of unconsolidated sediments accreted here later, which consequently also allowed northward expansion of the island (Fig. 4H3).

5.2. Century- and decadal-scale shoreline dynamics and sedimentation

5.2.1. Century scale shoreline dynamics

The centennial comparison of shorelines suggests that the island shape has evolved significantly since the late 19th century. The map from the hydrographic survey undertaken in 1897 (Fig. 3B) is in line with communications by locals stating that the southern island edge one century ago was located close to where the central sports field is found currently (Fig. 1C, 3C). This suggests that the W–E transect is close to the southern shoreline from the late 19th century when the island was more lens-shaped (Fig. 4M1) and significantly accreted in southward direction according to the locals in the 20th century (Fig. 4M2). Consequently, the samples A6 (3712 years cal BP) and A8 (3667 years cal BP) on the N–S transect must have been deposited significantly later than their radiocarbon ages imply. The radiocarbon dating of bulk samples thus represents maximum ages derived from the admixture of older components, with ages up to several millennia that have been reworked in the vicinity of the island or on the reef flat, as well as components that were only recently added to the sediment.

5.2.2. Decadal scale shoreline dynamics and sedimentation

The shoreline analysis from the recent decades reveals that the island is predominantly in an accreting state. Despite intermittent net area erosion between e.g. 2016 and 2017 (Fig. 3A, C), overall shoreline advance has led to a total island area of nearly 23 ha, indicating an increase of ~13 % over the past 24 years (Fig. 3). In the sediments that were deposited after 1999 according to this remote sensing analysis (i.e. the samples LK5-1, A1, A10, A11, A12, A31; Fig. 2A, B), coral and *Halimeda* are the dominant components. Although the radiocarbon dates of these sediments suggest pre-modern ages (e.g. A1 with 712 years cal BP and A31 with 1407 years cal BP), the satellite imagery data proves that their deposition took place within the last decades, thus implying that also reworked older sediments were deposited here (Fig. 2A, B). The increased abundance of *Halimeda* fragments in the modern shoreline sediments underlines however that they recently became a consistent and main constituent of the island sediments.

As summarized by Duvat (2018) shoreline studies in the Pacific and Indian Ocean found that islands larger than 10 ha are mainly stable (89 %) and a growth rate of >3 % area per decade is rare (11 %). Based on

this classification, the spatial expansion of a large island like Langkai at a rate of >5 % area per decade is particularly noteworthy. Due to the nearly equatorial location of the Spermonde Archipelago, the area is not affected by high-magnitude events such as cyclones, and thus the presumable drivers of island evolution are the reversing monsoon winds, as well as inter-seasonal fluctuations therein (Kench et al., 2009, 2023; Kench and Mann, 2017). Erosion in the past decades was limited to the eastern margin of Langkai, which faces monsoon winds during the boreal summer or dry season (Fig. 3C). This implies that erosion occurred mainly during the SE monsoon over the past two decades, with shoreline retreat rates of >1.0 m/year. Of note, the northeastern edge shows high dynamism and a net accretion indicating an active littoral transport zone, where sediment reworking is driven by wave refraction and diffraction over monsoonal changes in wave regimes (Mandlier and Kench, 2012; Kench and Mann, 2017). Likewise, accretion on the northwestern and southern margins has been promoted through alongshore sediment transport during SE monsoon. The near-constant accretion along the north, west and southern margins has led to a shift in the nodal position of the island, with the centroid migrating ~31 m toward the open ocean (Fig. 3C). Additionally, note that the empirical record of expansion of the island as documented in this study reflects the progradation of the edge of vegetation. Consequently, there is a lag between sediment influx onto the reef platform, deposition and subsequent expansion of the *vegetated* island core. Collectively, our data highlight that the island has maintained morphological stability and growth through the ecological transitions in the reef ecosystem that contribute to the development of the reef island (Fig. 4M3).

5.3. The increase of Halimeda in island sediments

Overall, the reef island sediments in the Spermonde Archipelago contain relatively higher proportions of *Halimeda* on the outer shelf, whereas mid-shelf islands usually have only scattered contributions of these green algae (Janßen et al., 2017; Kappelmann et al., 2023). This general trend can be explained by the fact that the outer shelf is exposed to seasonal upwelling and increased nutrient availability, which has been shown to promote *Halimeda* growth (Ilahude, 1970, 1978; Teichberg et al., 2013). Of significance, however, is that the proportions in the younger island sediments with >30 % of *Halimeda* contrast older deposits in our study and also exceed their content in surface sediments of other outer shelf islands, where *Halimeda* accounts for well below 10 % of the composition (Janßen et al., 2017). The trend toward *Halimeda*-dominated sediments over time (Figs. 2, 5E) suggests that the reefs around Langkai have shifted from a coral- to a more macroalgal-dominated state. Although the radiocarbon dates of this study do not exclude the possibility that *Halimeda* already became increasingly abundant already in the late Holocene, the sediments that have been deposited after 1999 according to the satellite imagery data (i.e. the samples LK5-1, A1, A10, A11, A12, A31), show an evident and consistent proportion of the macroalgae. Our sedimentological findings may thus be linked to a recent report on the reef status, in which the condition of the coral reefs around Langkai was rated as one of the worst in terms of living coral cover in the Spermonde Archipelago (Sari et al., 2021). Notably, the population on Langkai island has drastically increased over the second half of the 20th century from 10 permanent settled fishermen to >225 recent households, of which the majority work in fisheries (Gorris, 2016). Extensive and destructive fishing techniques such as cyanide and blast fishing emerged since the mid 20th century and are still common in the Spermonde Archipelago (Pet-Soede and Erdmann, 1998; Lampe et al., 2017), and specifically the Langkai reefs lack fishing policies (Sari et al., 2021). Such fishing methods impair the ability of e.g. parrotfish to maintain healthy coral growth, hence leading to the demise of the latter, and promoting shifts toward macroalgal reefs (Hughes, 1994; Cramer et al., 2017). Simultaneously, the decline of parrotfish, of which some species preferably feed on *Halimeda* (Mantyka and Bellwood, 2007), may also promote the long-term success of the algae, especially in upwelling settings (McNeil et al., 2021). Additional stress on the ecosystems may arise from nutrient enrichment through the discharge of untreated sewage waters from inhabited islands in Spermonde Archipelago (Edinger et al., 1998), as well as the mining of the solid coral framework for infrastructural use (Fig. 5A). Collectively, it appears that the local reef ecosystem is under modification already for several decades and thus are also the sediment production and island dynamics, probably as the result of combined natural and anthropogenic effects. Despite the pronounced ecosystem shift to macroalgal-dominance, the shoreline analysis of the past two decades provides evidence that the island is currently in an accretionary state, with significant increases of sand-sized *Halimeda* fragments (Fig. 4B). High sediment production of *Halimeda* is known from e.g. inter-reef areas in the Great Barrier Reef, where psammophytic species (attached to soft substrate) build extensive bioherms in water depths of >20 m (McNeil et al., 2020). In the shallow reefs around Langkai, growth of *Halimeda* was mainly observed on e.g. dead coral (Fig. 5B), suggesting that lithophytic (attached to solid substrate), non-bioherm-forming species are the main producers of *Halimeda* fragments (McNeil et al., 2020). Presumably the active reworking of sediment around Langkai does not allow the establishment of psammophytic *Halimeda* bioherms on soft substrates. Consequently, the dead solid coral framework would still serve as an important substrate for the settlement of *Halimeda*, and thus indirectly facilitate sediment production post mortem.

Our finding of a macroalgal-shift in island supplying ecosystems aligns with the report on the Spermonde Archipelago by Janßen et al. (2017), who found increased CCA in surface sediments on a mid-shelf island, interpreted as a consequence of increased anthropogenic pressures on reef ecosystems attributed to discharge of untreated sewage waters, nutrient enrichment and overfishing. In the *Halimeda*-rich sediments of our study, however, the proportions of CCA are commonly limited to 5 % or less. Although our study does not include a direct observation of the current calcifying biota in the ecosystems, we cannot exclude that CCA has increasingly spread in the degraded reefs of Langkai along with *Halimeda*, as observed elsewhere (Huntington et al., 2022; Cornwall et al., 2023). An explanation of the absence of CCA may be that their pathway into the sediment is mainly indirect, i.e. through bioerosion by (over-exploited) parrotfish, whereas segments of *Halimeda* are directly incorporated in the sediment upon death of the algae (Perry et al., 2011; Browne et al., 2021).

5.4. From an underestimated component to a potential key sediment source for reef islands?

Owing to their porous and platy structure, *Halimeda* fragments have a lower potential to withstand fragmentation under wave action at shorelines than other skeletal components, such as coral, bivalves and foraminifers (Ford and Kench, 2012; Morgan and Kench, 2016b). With estimates that up to 90 % of produced segments disintegrate into mud-sized (<63 μm) particles, this fragility compromises the suitability of *Halimeda* to contribute significantly to the maintenance of coastal systems and reef islands (Perry et al., 2016, 2020). In our present study however, *Halimeda* form the majority of recently deposited sand-sized sediments, hence constituting a major sediment source for the island accretion especially in the past two decades. The *Halimeda* fragments we have observed under the binocular microscope are almost exclusively fragmented and contain cements in their outer and inner pores. In order to visualize the effect these cements have on the internal structure we took SEM images from randomly selected *Halimeda* fragments from the samples A1 and A25. These confirm the presence of different degrees of cementation and crystal types within the macroalgal skeletons (e.g. Fig. 5C, D, see Supplementary materials S2 for additional SEM images). Wizemann et al. (2015) pointed out that the cementation in *Halimeda* can considerably enhance their preservation potential in reef sediments, and this internal cementation of *Halimeda* segments in

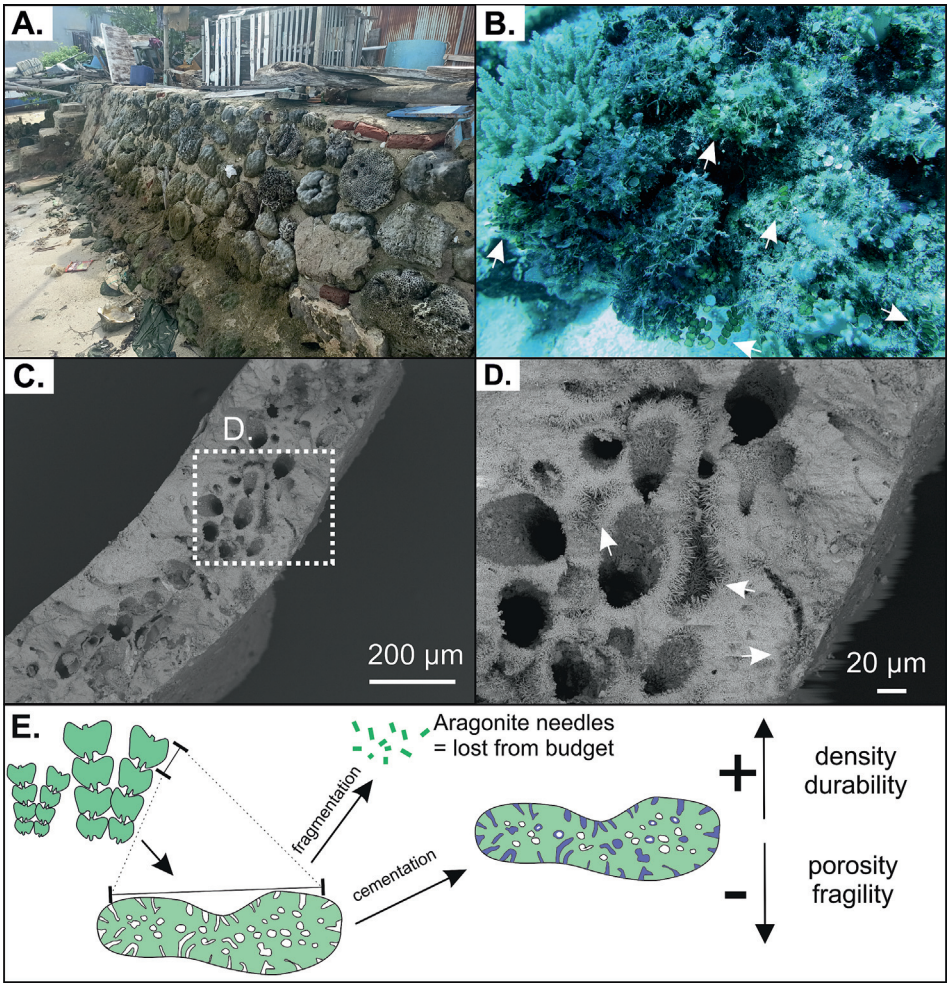

Fig. 5. A. Large coral blocks with diameters of around 20 to 40 centimeter used for the construction of infrastructure on the mid-shelf island Barrang Lompo, Spermonde Archipelago; Photo: Y. Kappelmann; B. prevailing settlement of algae on solid substrate in the reef of Langkai, *Halimeda* marked with arrows; image width approximately 1.2 m; Photo: M. Stuhr; C. SEM backscatter image of *Halimeda* fragment from sample A1; D. SEM backscatter image of the area marked in C. showing abundant growth of internal cements in the pore space marked with arrows; E. conceptual model of sediment production by *Halimeda* and the effect of internal cementation.

shallow marine environments may take place in <100 years (Mann et al., 2021). The internal cementation effectively decreases the porosity, therefore preventing individual segments from breakdown into mud-sized aragonite needles (Fig. 5E). We assume that early-diagenetic cementation in porous *Halimeda* segments is a probable factor in their preservation and may be enabled, when the individual segments remain in a low-energetic setting for a sufficient amount of time (Wizemann et al., 2015). Overall, given that the *Halimeda*-shift around Langkai has likely intensified since the mid 20th century, the cementation may take place even faster, i.e. within decades, and may facilitate long-term preservation of the fragments within the reef and island sediments.

We argue that the process of cementation has implications for the global perspective on carbonate budgets. Bleaching events and coral reef degradation due to local anthropogenic stressors (e.g., increased nutrient influx, overfishing), have been increasingly recorded since the late 20th century and their extent has increased ever since, with proposed shifts to macroalgal-dominated states, which in several cases are characterized by increased *Halimeda* growth (Hughes et al., 2017, 2018; Perry et al., 2020; Fukunaga et al., 2022). Given that these bleaching events are recent events, their mid- to long-term effects on sedimentary systems are not yet understood. Therefore, our study provides an example of how coastal systems react to coral-macroalgal shifts. We hypothesize that *Halimeda* settlement on degraded reefs is a valuable source to provide suitable sediment for coastal sedimentary systems. This may in particular be the case in regions of low storm frequency, where reef islands consist predominantly of sand-sized sediments (Woodroffe, 2008). In order to enhance our understanding of the potential of *Halimeda* production for island sediment supply, it is however necessary to further investigate (1) the ratio of segment breakdown vs segment survival that enables later cementation, (2) the physico-chemical drivers of cementation and (3) the related time frames over which internal cementation is taking place as summarized in Fig. 5E. Furthermore, our study clearly underlines the importance of coupling remote sensing data to sedimentological field data, in order to shed light on the ecological component of reported island dynamics.

6. Conclusion

In our study we present a model of Holocene reef island formation in the Spermonde Archipelago and reveal its shoreline dynamics in the recent decades. We find that the sea-level fall in the mid-Holocene has promoted the evolution of a low-energetic backreef environment in which a greater variety of sediment producing species found habitats, whose skeletal remains then contributed to the formation of the island. This is shown by a shift in the sediment composition with increased proportions of gastropods, *Halimeda* and foraminifera, compared to underlying coral sediments. The more diverse sediments were deposited after a sea-level fall and the subsequent stabilization of the same around 4200 years cal BP. These findings underline that sea-level fluctuations

affect the production of reef derived carbonate, and thus the development of landforms.

Our analysis of shoreline evolution suggests, that the island has adjusted its shorelines steadily since the 19th century and that accretion was dominant over the past decades, resulting in an island area increase of 13 % since 1999. Importantly, this accretion was supported by *Halimeda*-rich sediments, whereas older deposits were mainly formed by coral-dominated sediments. The evident shift in the sedimentological composition is presumably the result of natural nutrient supply through upwelling, and intensified lately with increasing anthropogenic pressure on the coral reef ecosystems that came along with intensive settlement of the island and increased exploitation of its surrounding coral reefs. Our findings hence prove that the sediment sources of the island were altered and still provide sufficient material for island growth despite a macroalgal shift in the surrounding reef ecosystem. Given that this pronounced ecosystem shift has seemingly affected the sediment supplying reef ecosystems more drastically since the mid 20th century, our study provides an exceptional analog of how reef islands may react to the currently increasing coral- to macroalgal-shifts in the mid-term (i.e. on a scale of several decades), when increased carbonate production is provided by the green algae *Halimeda*. This potentially opens new approaches to coastal management of reef islands.

CRediT authorship contribution statement

Yannis Kappelmann: Conceptualization, Data curation, Formal analysis, Investigation, Methodology, Visualization, Writing – original draft, Writing – review & editing. **Meghna Sengupta:** Data curation, Formal analysis, Visualization, Writing – review & editing. **Thomas Mann:** Conceptualization, Funding acquisition, Methodology, Project administration, Resources, Supervision, Writing – review & editing. **Marleen Stuhr:** Project administration, Writing – review & editing. **Dominik Kneer:** Resources, Writing – review & editing. **Jamaluddin Jompa:** Writing – review & editing. **Hildegard Westphal:** Conceptualization, Funding acquisition, Methodology, Project administration, Resources, Supervision, Writing – review & editing.

Data availability

The data used for the present study are available from the PANGAEA data repository under https://doi.org/10.1594/PANGAEA.967719 (Kappelmann et al., 2024).

Declaration of competing interest

The authors declare that they have no known competing financial interests or personal relationships that could have appeared to influence the work reported in this paper.

Acknowledgments

This study and the doctoral student position of Y.K. were funded through a grant from the Deutsche Forschungsgemeinschaft (DFG; grant No. MA6967/2-1) in the SPP 1889 "Regional Sea Level and Society (SeaLevel)" received by T.M. This study is part of a cooperation between the Hasanuddin University (UNHAS), Indonesia, and the Leibniz Centre for Tropical Marine Research (ZMT), Germany. The field work in 2016 was enabled under the research permit No. 36/EXT/SIP/FRP/SM/VII/2015 by the Indonesian Ministry of Research and Technology (RisTek), funded by the German Ministry for Education and Research (BmBF; grant No. 03F0642A) and further financially supported by the Alfred-Wegener-Institute, Helmholtz Centre for Polar and Marine Research (AWI), Germany. The field work in 2021 was facilitated under the research permit No. 72/SKET/DIK/03/2020/10 by the Embassy of the Republic of Indonesia, Berlin, Germany. Me. S. was funded by the Alexander von Humboldt Foundation.

We thank the local community of the island Pulau Langkai for providing permission for scientific fieldwork, hospitability and useful reports of the island morphodynamical history. We also thank Andi Eka Puji Pratiwi, Ridwan and Edi Kukang for assisting the field work. Laboratory facilities were provided by the Leibniz Centre for Tropical Marine Research (ZMT). We acknowledge the technical and laboratory support by Sebastian Flotow. Moreover, we thank the editor Dr. Giorgio Basilici and the two anonymous reviewers who have provided constructive and thoughtful comments to improve this manuscript.

Appendix A. Supplementary data

Supplementary data to this article can be found online at https://doi.org/10.1016/j.sedgeo.2024.106675.

References

Bender, M., Mann, T., Stocchi, P., Kneer, D., Schöne, T., Illigner, J., Jompa, J., Rovere, A., 2020. Late Holocene (0–6 ka) sea-level changes in the Makassar Strait, Indonesia. Climate of the Past 16, 1187–1205.

Blott, S.J., Pye, K., 2001. GRADISTAT: a grain size distribution and statistics package for the analysis of unconsolidated sediments. Earth Surface Processes and Landforms 26, 1237–1248.

Bronk Ramsey, C., 2009. Bayesian analysis of radiocarbon dates. Radiocarbon 51, 337–360.

Browne, N.K., Cuttler, M., Moon, K., Morgan, K., Ross, C.L., Castro-Sanguino, C., Kennedy, E., Harris, D., Barnes, P., Bauman, A., Beetham, E., Bonesso, J., Bozec, Y.-M., Cornwall, C., Dee, S., DeCarlo, T., D'Olivo, J.P., Doropoulos, C., Evans, R.D., Eyre, B., Gatenby, P., Gonzalez, M., Hamylton, S., Hansen, J., Lowe, R., Mallela, J., O'Leary, M., Roff, G., Saunders, B.J., Zweilfer, A., 2021. Predicting responses of geo-ecological carbonate reef systems to climate change: a conceptual model and review. In: J, H.S., Lemasson, A.J., Allcock, A.L., Bates, A.E., Byrne, M., Evans, A.J., Firth, L.B., Marzinelli, E.M., Russell, B.D., Smith, I.P., Swearer, S.E., Todd, P.A. (Eds.), Oceanography and Marine Biology: An Annual Review. CRC Press, Taylor & Francis, London, United Kingdom, pp. 229–370.

Cornwall, C.E., Carlot, J., Branson, O., Courtney, T.A., Harvey, B.P., Perry, C.T., Andersson, A.J., Diaz-Pulido, G., Johnson, M.D., Kennedy, E., Krieger, E.C., Mallela, J., McCoy, S.J., Nugues, M.M., Quinter, E., Ross, C.L., Ryan, E., Saderne, V., Comeau, S., 2023. Crustose coralline algae can contribute more than corals to coral reef carbonate production. Communications Earth & Environment 4, 105. https://doi.org/10.1038/s43247-023-00766-w.

Cramer, K.L., O'Dea, A., Clark, T.R., Zhao, J.X., Norris, R.D., 2017. Prehistorical and historical declines in Caribbean coral reef accretion rates driven by loss of parrotfish. Nature Communications 8, 14160. https://doi.org/10.1038/ncomms14160.

Cuttler, M.V., Vos, K., Branson, P., Hansen, J.E., O'leary, M., Browne, N.K., Lowe, R.J., 2020. Interannual response of reef islands to climate-driven variations in water level and wave climate. Remote Sensing 12, 4089. https://doi.org/10.3390/rs12244089.

Ding, X., Bassinot, F., Guichard, F., Fang, N.Q., 2013. Indonesian Throughflow and monsoon activity records in the Timor Sea since the last glacial maximum. Marine Micropaleontology 101, 115–126.

Done, T.J., 1982. Coral zonation: its nature and significance. In: Barnes, D.J. (Ed.), Perspectives on Coral ReefsAustralian Institute of Marine Science (AIMS), Townsville, Australia, pp. 107–147.

Duvat, V.K.E., 2018. A global assessment of atoll island planform changes over the past decades. WIREs Climate Change 10, e557. https://doi.org/10.1002/wcc.557.

East, H.K., Perry, C.T., Kench, P.S., Liang, Y., 2016. Atoll-scale comparisons of the sedimentary structure of coral reef rim islands, Huvadhu Atoll, Maldives. Journal of Coastal Research 75, 577–581.

Edinger, E.N., Jompa, J., Limmon, G.V., Widjatmoko, W., Risk, M.J., 1998. Reef degradation and coral biodiversity in Indonesia: effects of land-based pollution, destructive fishing practices and changes over time. Marine Pollution Bulletin 36, 617–630.

Ford, M.R., Kench, P.S., 2012. The durability of bioclastic sediments and implications for coral reef deposit formation. Sedimentology 59, 830–842.

Fukunaga, A., Burns, J.H.R., Pascoe, K.H., Kosaki, R.K., 2022. A remote coral reef shows macroalgal succession following a mass bleaching event. Ecological Indicators 142, 109175. https://doi.org/10.1016/j.ecolind.2022.109175.

Glaser, M., Breckwoldt, A., Deswandi, R., Radjawali, I., Baitoningsih, W., Ferse, S.C.A., 2015. Of exploited reefs and fishers – a holistic view on participatory coastal and marine management in an Indonesian archipelago. Ocean and Coastal Management 116, 193–213.

Gordon, A.L., Napitu, A., Huber, B.A., Gruenburg, L.K., Pujiana, K., Agustiadi, T., Kuswardani, A., Mbay, N., Setiawan, A., 2019. Makassar Strait throughflow seasonal and interannual variability: an overview. Journal of Geophysical Research: Oceans 124, 3724–3736.

Gorris, P., 2016. Deconstructing the reality of community-based management of marine resources in a small island context in Indonesia. Frontiers in Marine Science 3, 120. https://doi.org/10.3389/fmars.2016.00120.

Hall, R., Cloke, I.R., Nur'aini, S., Puspita, S.D., Calvert, S.J., Elders, C.F., 2009. The North Makassar Straits: what lies beneath? Petroleum Geoscience 15, 147–158.

Heaton, T.J., Köhler, P., Butzin, M., Bard, E., Reimer, R.W., Austin, W.E., Ramsey, C.B., Grootes, P.M., Hughen, K.A., Kromer, B., 2020. Marine20—the marine radiocarbon age calibration curve (0–55,000 cal BP). Radiocarbon 62, 779–820.

Hoegh-Guldberg, O., Mumby, P.J., Hooten, A.J., Steneck, R.S., Greenfield, P., Gomez, E., Harvell, C.D., Sale, P.F., Edwards, A.J., Caldeira, K., Knowlton, N., Eakin, C.M., Iglesias-

Prieto, R., Muthiga, N., Bradbury, R.H., Dubi, A., Hatziolos, M.E., 2007. Coral reefs under rapid climate change and ocean acidification. Science 318, 1737–1742.
Hoeksema, B.W., 2012. Distribution patterns of mushroom corals (Scleractinia: Fungiidae) across the Spermonde Shelf, South Sulawesi. The Raffles Bulletin of Zoology 60, 183–212.
Hughes, T.P., 1994. Catastrophes, phase shifts, and large-scale degradation of a Caribbean coral reef. Science 265, 1547–1551.
Hughes, T.P., Barnes, M.L., Bellwood, D.R., Cinner, J.E., Cumming, G.S., Jackson, J.B.C., Kleypas, J., van de Leemput, I.A., Lough, J.M., Morrison, T.H., Palumbi, S.R., van Nes, E.H., Scheffer, M., 2017. Coral reefs in the Anthropocene. Nature 546, 82–90.
Hughes, T.P., Anderson, K.D., Connolly, S.R., Heron, S.F., Kerry, J.T., Lough, J.M., Baird, A.H., Baum, J.K., Berumen, M.L., Bridge, T.C., Claar, D.C., Eakin, C.M., Gilmour, J.P., Graham, N.A.J., Harrison, H., Hobbs, J.P.A., Hoey, A.S., Hoogenboom, M., Lowe, R.J., McCulloch, M.T., Pandolfi, J.M., Pratchett, M., Schoepf, V., Torda, G., Wilson, S.K., 2018. Spatial and temporal patterns of mass bleaching of corals in the Anthropocene. Science 359, 80–83.
Huntington, B., Weible, R., Halperin, A., Winston, M., McCoy, K., Amir, C., Asher, J., Vargas-Angel, B., 2022. Early successional trajectory of benthic community in an uninhabited reef system three years after mass coral bleaching. Coral Reefs 41, 1087–1096.
Husband, E., East, H.K., Hocking, E.P., Guest, J., 2023. Honduran Reef Island shoreline change and planform evolution over the last 15 years: implications for reef island monitoring and futures. Remote Sensing 15, 4787. https://doi.org/10.3390/rs15194787.
Ilahude, A.G., 1970. On the occurrence of Upwelling in the Southern Makassar Strait. Marine Research in Indonesia 10, 3–53.
Ilahude, A.G., 1978. On the factors affecting the productivity of the Southern Makassar Strait. Marine Research in Indonesia 21, 81–107.
Janßen, A., Wizemann, A., Klicpera, A., Satari, D.Y., Westphal, H., Mann, T., 2017. Sediment composition and facies of coral reef islands in the Spermonde Archipelago, Indonesia. Frontiers in Marine Science 4, 144. https://doi.org/10.3389/fmars.2017.00144.
Kappelmann, Y., Westphal, H., Kneer, D., Wu, H.C., Wizemann, A., Jompa, J., Mann, T., 2023. Fluctuating sea-level and reversing Monsoon winds drive Holocene lagoon infill in Southeast Asia. Scientific Reports 13, 5042. https://doi.org/10.1038/s41598-023-31976-z.
Kappelmann, Y., Sengupta, M., Mann, T., Stuhr, M., Kneer, D., Jompa, J., Westphal, H., 2024. Sedimentological and remote sensing data from the reef island Langkai, Spermonde Archipelago, Indonesia (dataset bundled publication). PANGAEA https://doi.org/10.1594/PANGAEA.967719.
Kench, P.S., Mann, T., 2017. Reef island evolution and dynamics: insights from the Indian and Pacific Oceans and perspectives for the Spermonde Archipelago. Frontiers in Marine Science 4, 145. https://doi.org/10.3389/fmars.2017.00145.
Kench, P.S., Parnell, K.E., Brander, R.W., 2009. Monsoonally influenced circulation around coral reef islands and seasonal dynamics of reef island shorelines. Marine Geology 266, 91–108.
Kench, P., Smithers, S., McLean, R., 2012. Rapid reef island formation and stability over an emerging reef flat: Bewick Cay, northern Great Barrier Reef, Australia. Geology 40, 347–350.
Kench, P.S., Owen, S.D., Beetham, E.P., Mann, T., McLean, R.F., Ashton, A., 2020. Holocene sea level dynamics drive formation of a large atoll island in the central Indian Ocean. Global and Planetary Change 195, 103354. https://doi.org/10.1016/j.gloplacha.2020.103354.
Kench, P.S., Liang, C., Ford, M.R., Owen, S.D., Aslam, M., Ryan, E.J., Turner, T., Beetham, E., Dickson, M.E., Stephenson, W., Vila-Concejo, A., McLean, R.F., 2023. Reef islands have continually adjusted to environmental change over the past two millennia. Nature Communications 14, 508. https://doi.org/10.1038/s41467-023-36171-2.
Lampe, M., Demmalino, E.B., Neil, M., Jompa, J., 2017. Main drivers and alternative solutions for destructive fishing in South Sulwaesi-Indonesia: lessons learned from Spermonde Archipelago, Taka Bonerate, and Sembilan Island. Science International (Lahore) 29, 159–164.
Liang, Y., Kench, P.S., Ford, M.R., East, H.K., 2016. Lagoonal reef sediment supply and island connectivity, Huvadhu Atoll, Maldives. Journal of Coastal Research 75, 587–591.
Mandlier, P.G., Kench, P.S., 2012. Analytical modelling of wave refraction and convergence on coral reef platforms: implications for island formation and stability. Geomorphology 159-160, 84–92.
Mann, T., Rovere, A., Schöne, T., Klicpera, A., Stocchi, P., Lukman, M., Westphal, H., 2016. The magnitude of a mid-Holocene sea-level highstand in the Strait of Makassar. Geomorphology 257, 155–163.
Mann, T., Wizemann, A., Stuhr, M., Kappelmann, Y., Janßen, A., Jompa, J., Westphal, H., 2021. Shallow-marine carbonate cementation in Holocene segments of the calcifying green alga Halimeda. Sedimentology 69, 282–300.
Mantyka, C.S., Bellwood, D.R., 2007. Macroalgal grazing selectivity among herbivorous coral reef fishes. Marine Ecology Progress Series 352, 177–185.
McKoy, H., Kennedy, D.M., Kench, P.S., 2010. Sand cay evolution on reef platforms, Mamanuca Islands, Fiji. Marine Geology 269, 61–73.
McNeil, M.A., Nothdurft, L.D., Dyriw, N.J., Webster, J.M., Beaman, R.J., 2020. Morphotype differentiation in the Great Barrier Reef Halimeda bioherm carbonate factory: internal architecture and surface geomorphometrics. The Depositional Record 7, 176–199.
McNeil, M., Nothdurft, L., Erler, D., Hua, Q., Webster, J.M., 2021. Variations in Mid- to Late Holocene nitrogen supply to Northern Great Barrier Reef Halimeda macroalgal bioherms. Paleoceanography and Paleoclimatology 36, e2020PA003871. https://doi.org/10.1029/2020PA003871.
Mohtadi, M., Oppo, D.W., Steinke, S., Stuut, J.-B.W., De Pol-Holz, R., Hebbeln, D., Lückge, A., 2011. Glacial to Holocene swings of the Australian–Indonesian monsoon. Nature Geoscience 4, 540–544.
Morgan, K.M., Kench, P.S., 2016a. Parrotfish erosion underpins reef growth, sand talus development and island building in the Maldives. Sedimentary Geology 341, 50–57.
Morgan, K.M., Kench, P.S., 2016b. Reef to island sediment connections on a Maldivian carbonate platform: using benthic ecology and biosedimentary depositional facies to examine island-building potential. Earth Surface Processes and Landforms 41, 1815–1825.
Neumann, A.C., Macintyre, I.G., Reef response to sea-level rise: keep-up, catch-up or give-up. C. Gabrie, J.L. Toffart, B. Salvat (Ed.), Proceedings of the Fifth International Coral Reef Congress Tahiti. 27 May-1 June 1985, Moorea, French Polynesia. Antenne Museum-EPHE, pp. 105–110.
Perry, C.T., Kench, P.S., Smithers, S.G., Riegl, B., Yamano, H., O'Leary, M.J., 2011. Implications of reef ecosystem change for the stability and maintenance of coral reef islands. Global Change Biology 17, 3679–3696.
Perry, C.T., Murphy, G.N., Kench, P.S., Smithers, S.G., Edinger, E.N., Steneck, R.S., Mumby, P.J., 2013. Caribbean-wide decline in carbonate production threatens coral reef growth. Nature Communications 4, 1402. https://doi.org/10.1038/ncomms2409.
Perry, C.T., Kench, P.S., O'Leary, M.J., Morgan, K.M., Januchowski-Hartley, F., 2015. Linking reef ecology to island building: parrotfish identified as major producers of island-building sediment in the Maldives. Geology 43, 503–506.
Perry, C.T., Morgan, K.M., Salter, M.A., 2016. Sediment generation by Halimeda on atoll interior coral reefs of the southern Maldives: a census-based approach for estimating carbonate production by calcareous green algae. Sedimentary Geology 346, 17–24.
Perry, C.T., Morgan, K.M., Lange, I.D., Yarlett, R.T., 2020. Bleaching-driven reef community shifts drive pulses of increased reef sediment generation. Royal Society Open Science 7, 192153. https://doi.org/10.1098/rsos.192153.
Pet-Soede, L., Erdmann, M.V., 1998. Blast fishing in southwest Sulawesi, Indonesia. NAGA, The ICLARM Quarterly. vol. 20, pp. 4–9.
Sari, N.W.P., Siringoringo, R.M., Abrar, M., Putra, R.D., Sutiadi, R., Yusuf, S., 2021. Status of coral reefs in the water of Spermonde, Makassar, South Sulawesi. E3S Web of Conferences vol. 324, 03007. https://doi.org/10.1051/e3sconf/202132403007.
Scoffin, T., 1993. The geological effects of hurricanes on coral reefs and the interpretation of storm deposits. Coral Reefs 12, 203–221.
Sengupta, M., Ford, M.R., Kench, P.S., Perry, G.L.W., 2023. Drivers of shoreline change on Pacific coral reef islands: linking island change to processes. Regional Environmental Change 23, 110. https://doi.org/10.1007/s10113-023-02103-5.
Stoddart, D., Steers, J., 1977. Chapter 3: the nature and origin of coral reef islands. In: Jones, O.A., Endean, R. (Eds.), Biology and Geology of Coral Reefs. Academic Press, London, United Kingdom, pp. 59–105.
Storlazzi, C.D., Gingerich, S.B., van Dongeren, A., Cheriton, O.M., Swarzenski, P.W., Quataert, E., Voss, C.I., Field, D.W., Annamalai, H., Piniak, G.A., McCall, R., 2018. Most atolls will be uninhabitable by the mid-21st century because of sea-level rise exacerbating wave-driven flooding. Science Advances 4, eaap9741. https://doi.org/10.1126/sciadv.aap9741.
Teichberg, M., Fricke, A., Bischof, K., 2013. Increased physiological performance of the calcifying green macroalga Halimeda opuntia in response to experimental nutrient enrichment on a Caribbean coral reef. Aquatic Botany 104, 25–33.
Thieler, E.R., Himmelstoss, E.A., Zichichi, J.L., Ergul, A., 2009. The Digital Shoreline Analysis System (DSAS) version 4.0 — an ArcGIS extension for calculating shoreline change. Open-File Report 2008-1278. US Geological Survey, Reston, VA.
Umbgrove, J.H.F., 1928. De koraalriffen van den Spermonde-Archipel (Zuid-Celebes). Leidse Geologische Medelingenvol. 3, pp. 228–247.
Webb, A.P., Kench, P.S., 2010. The dynamic response of reef islands to sea-level rise: evidence from multi-decadal analysis of island change in the Central Pacific. Global and Planetary Change 72, 234–246.
Wentworth, C.K., 1922. A scale of grade and class terms for clastic sediments. The Journal of Geology 30, 377–392.
Westphal, H., Murphy, G.N., Doo, S.S., Mann, T., Petrovic, A., Schmidt, C., Stuhr, M., 2022. Ecosystem design as an avenue for improving services provided by carbonate producing marine ecosystems. PeerJ 10, e12785. https://doi.org/10.7717/peerj.12785.
Wijsman-Best, M., Moll, H., de Klerk, L.G., 1981. Present status of the coral reefs in the Spermonde Archipelago (South Sulawesi, Indonesia). In: Gomez, E.D., Birkeland, C.E. (Eds.), Proceedings of the Fourth International Coral Reef Symposium. 18–22 May 1981. University of Philippines, Manila, Phillippines, pp. 263–267.
Wizemann, A., Mann, T., Klicpera, A., Westphal, H., 2015. Microstructural analyses of sedimentary Halimeda segments from the Spermonde Archipelago (SW Sulawesi, Indonesia): a new indicator for sediment transport in tropical reef islands? Facies 61, 4. https://doi.org/10.1007/s10347-015-0429-5.
Woodroffe, C.D., 2008. Reef-island topography and the vulnerability of atolls to sea-level rise. Global and Planetary Change 62, 77–96.
Woodroffe, C., Morrison, R., 2001. Reef-island accretion and soil development on Makin, Kiribati, central Pacific. Catena 44, 245–261.
Woodroffe, C.D., McLean, R.F., Smithers, S.G., Lawson, E.M., 1999. Atoll reef-island formation and response to sea-level change: West Island, Cocos (Keeling) Islands. Marine Geology 160, 85–104.
Woodroffe, C.D., Farrell, J.W., Hall, F.R., Harris, P., 2017. Calcium carbonate production and contribution to coastal sediments. In: Nations, U. (Ed.), The First Global Integrated Marine Assessment: World Ocean Assessment I. Cambridge University Press, Cambridge, pp. 149–157.
Yamano, H., Miyajima, T., Koike, I., 2000. Importance of foraminifera for the formation and maintenance of a coral sand cay: Green Island, Australia. Coral Reefs 19, 51–58.
Yamano, H., Kayanne, H., Yonekura, N., 2001. Anatomy of a modern coral reef flat: a recorder of storms and uplift in the late Holocene. Journal of Sedimentary Research 71, 295–304.